iScience

CellPress
OPEN ACCESS

Article

Memory ability and retention performance relate differentially to sleep depth and spindle type

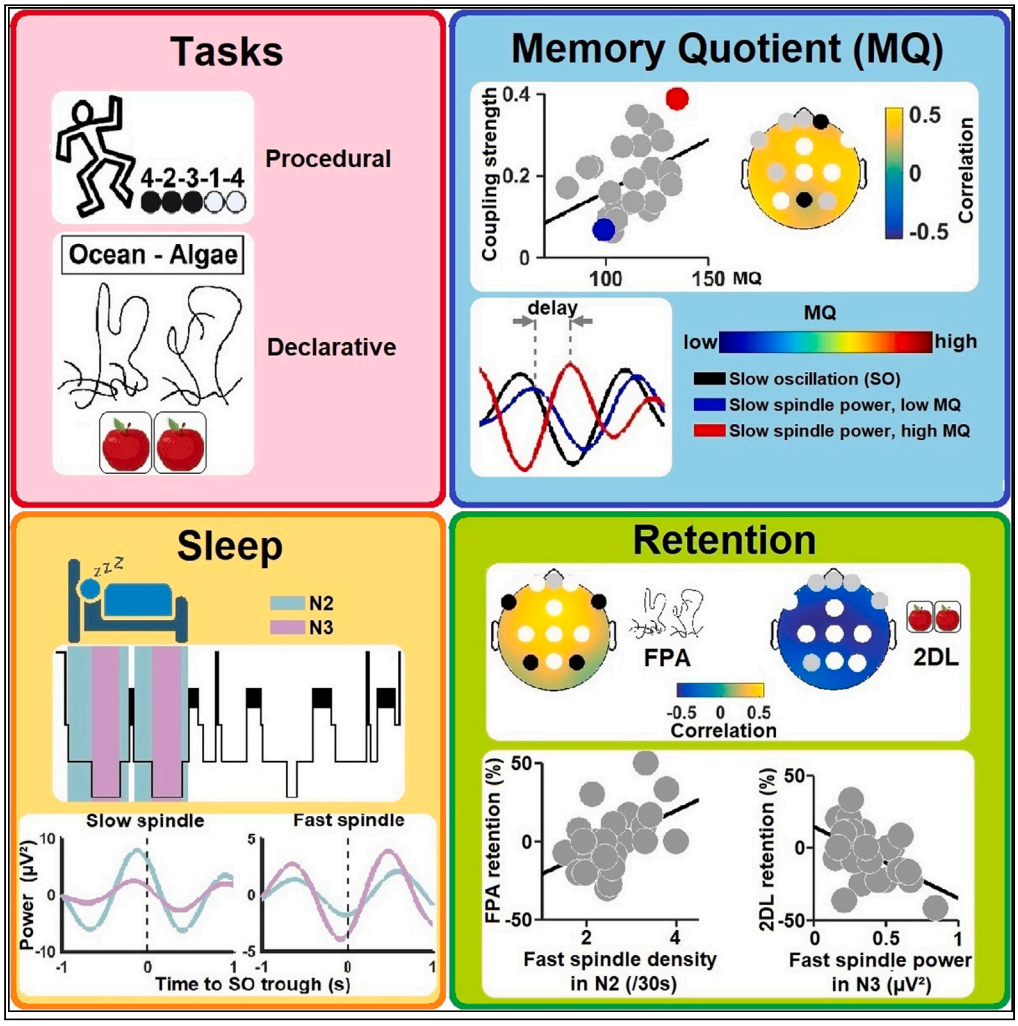

Fereshteh Dehnavi, Ping Chai Koo-Poeggel, Maryam Ghorbani, Lisa Marshall

maryamgh@um.ac.ir (M.G.)
lisa.marshall@uni-luebeck.de (L.M.)

Highlights

Slow oscillation-slow spindle coupling in post-task sleep predicts memory ability

Memory retention relates oppositely with fast spindle activity in N2 versus N3

The relationship of fast spindles to retention depends on task type and sleep depth

Slow oscillation-fast spindle coupling correlates with procedural memory retention

Dehnavi et al., iScience 26, 108154
November 17, 2023
https://doi.org/10.1016/j.isci.2023.108154

iScience

CellPress
OPEN ACCESS

Article

Memory ability and retention performance relate differentially to sleep depth and spindle type

Fereshteh Dehnavi,[1,5] Ping Chai Koo-Poeggel,[2,3] Maryam Ghorbani,[1,4,5,*] and Lisa Marshall[2,3,6,*]

SUMMARY

Temporal interactions between non-rapid eye movement (NREM) sleep rhythms especially the coupling between cortical slow oscillations (SO, ~1 Hz) and thalamic spindles (~12 Hz) have been proposed to contribute to multi-regional interactions crucial for memory processing and cognitive ability. We investigated relationships between NREM sleep depth, sleep spindles and SO-spindle coupling regarding memory ability and memory consolidation in healthy humans. Findings underscore the functional relevance of spindle dynamics (slow versus fast), SO-phase, and most importantly NREM sleep depth for cognitive processing. Cross-frequency coupling analyses demonstrated stronger precise temporal coordination of slow spindles to SO down-state in N2 for subjects with higher general memory ability. A GLM model underscored this relationship, and furthermore that fast spindle properties were predictive of overnight memory consolidation. Our results suggest cognitive fingerprints dependent on conjoint fine-tuned SO-spindle temporal coupling, spindle properties, and brain sleep state.

INTRODUCTION

Non-rapid eye movement (NREM) sleep is composed of many different shades. As sleep deepens, sleep spindles commence, density and magnitude of sleep slow oscillations (SO) increase. With further deepening of NREM sleep density of thalamo-cortical spindles and also their frequency tend to decrease.[1–3] According to the concept of active systems consolidation, the reactivation during sleep of neural networks active during preceding learning facilitates information transfer between and within brain structures.[4] The electrophysiological activity potentially mediating cellular and molecular changes for memory storage appear to be reflected in the coalescence of sleep slow oscillations, thalamo-cortical sleep spindles and/or hippocampal sharp-wave ripples.[5–8] In the EEG such inter-regional interaction is well assessed by SO-spindle coupling. At least two types of fast oscillatory events are distinguished, fast and slow sleep spindles.[5,9–13] Aside from frequency, neurophysiological distinctions between these spindle types are indicated by their EEG topography, pharmacological dependence, and current source density distributions.[5,9,14–19] Notably, spindle frequency bands often differ between research groups, e.g., as a function of detection method,[9,20] and debatable intracortical (laminar) distribution.[21,22] In EEG and MEG fast spindles couple to the depolarizing SO Up state or down-to-up state transition, and slow spindles couple to the SO Up-to-down state, revealing stable individual differences across nights.[11,12,23]

Interestingly, despite indications for multiple evidence pointing toward qualitatively differential kinds of processing during light and deep NREM sleep,[12,24–30] only recently are the spindle types at different NREM sleep depths or in relation to SO occurrence[31,32] investigated together with functional correlates of sleep spindles.[20,31–37]

Sleep spindle parameters and topographic distribution have been investigated as correlates of pre-sleep task learning e.g.,[38,39] memory retention and reactivation processes during the sleep period reviewed in.[5,40,41] The latter has received strong support by the upsurge of targeted memory reactivation and related studies,[42–44] although not uncontroversial.[45] These relationships of spindles to experience-dependent activity is confounded by inter-individual differences, most notably by measures of general mental ability,[26,34,46,47] but also sex and age.[18,20,48–50]

The aim of the present article is to firstly disclose differences, dependent upon pre-sleep learning, on individually determined slow and fast spindle properties (spindle density, power and coupling to the slow oscillation) separately during N2 and N3 sleep. For this we compared spindle properties after subjects conducted a battery of declarative and procedural learning tasks versus a non-learning control session. On this basis, we secondly, investigate whether the trait-like general memory quotient of the subjects is associated with any of the above spindle properties. Previously the general memory quotient of these subjects correlated with the efficacy of non-invasive brain stimulation

[1]Department of Electrical Engineering, Ferdowsi University of Mashhad, Mashhad 9177948974, Iran
[2]Institute of Experimental and Clinical Pharmacology and Toxicology, University of Luebeck, Ratzeburger Allee 160, Bldg. 66, 23562 Luebeck, Germany
[3]Center for Brain, Behavior and Metabolism, University of Luebeck, 23562 Luebeck, Germany
[4]Rayan Center for Neuroscience and Behavior, Ferdowsi University of Mashhad, Mashhad 9177948974, Iran
[5]Center for International Scientific Studies & Collaborations (CISSC), Shahid Azodi Street, Karim-Khane Zand Boulevard, Tehran 15875-7788, Iran
[6]Lead contact
*Correspondence: maryamgh@um.ac.ir (M.G.), lisa.marshall@uni-luebeck.de (L.M.)
https://doi.org/10.1016/j.isci.2023.108154

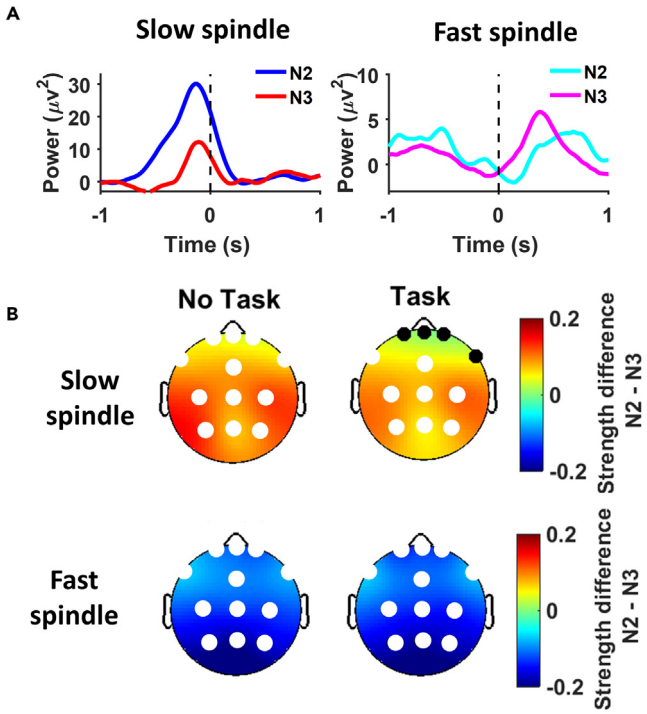

Figure 1. SO spindle coupling strength changes differentially for slow and fast spindles with NREM sleep depth

(A) Slow (Left) and fast (Right) spindle wavelet power locked to SO negative half-wave peak (t = 0 s) for Fz and Cz, respectively in N2 and N3 averaged across all subjects.

(B) Topographical distribution of the difference in SO-spindle coupling strength between N2 and N3 for slow (Top) and fast (Bottom) spindles in both the No Task and Task conditions for all subjects (n = 24 and 25 for SO-slow and fast spindle coupling, respectively). Electrodes belonging to the cluster with a significant difference between N2 and N3 (nonparametric cluster-permutation statistics, slow spindle: $p < 0.001$ and $p = 0.003$ for No Task and Task conditions, respectively, fast spindle: $p < 0.001$ and $p < 0.001$ for No Task and Task conditions, respectively) are indicated by white dots ($p < 0.05$). For $p > 0.1$, black dots (paired t-tests).

on overnight consolidation of a declarative task.[34] We include a general linear model to investigate the predictive value of spindle and coupling parameters for the assessed memory quotient. Our long-term aspiration is to determine (spindle) parameters relevant for predicting the efficacy of non-invasive brain stimulation on memory retention.

RESULTS

Slow oscillations spindle coupling strength changes differentially for slow and fast spindles with non-rapid eye movement sleep depth

Results of the within-subject repeated measures (rm) ANOVA for SO-slow and SO-fast spindle coupling strength with the factors Stage and Topography are given in Tables S1–S4. SO-slow spindle coupling strength was significantly stronger in N2 than N3 in both Task and No-Task conditions (Figure 1; Tables S1 and S2), with absence of a main Topography effect in the Task condition. In contrast to SO-slow spindle coupling, SO-fast spindle coupling strength was stronger in N3 than N2 with this effect widely distributed across frontal to posterior locations also in both conditions (Figure 1; Tables S3 and S4).

Mean fast and slow spindle power, revealed the characteristic topographical distribution for No Task, with higher mean in fronto-central power for slow spindles, and higher centro-parietal power for fast spindles (Tables S2, S4, and Figure S1). Comparisons of NREM sleep depth revealed over the frontal region significantly lower slow spindle power in N2 than N3 (FP1, FPz, FP2, F7 and Fz, $p = 0.034$, cluster-based permutation). Slow spindle density was similarly significantly lower in N2 than N3 over frontal regions (for FP1, FPz, FP2, F7, Fz and F8, $p = 0.014$, cluster-based permutation test) while it was significantly higher in N2 than N3 over parietal regions (for P3, Pz and P4, $p = 0.044$, cluster-based permutation test). Expectedly, fast spindle power and density were significantly larger in N2 than N3 at all electrodes ($p < 0.001$, cluster-based permutation test; Figure S1). Amount of time spent in the NREM sleep stages N2 and N3 did not differ significantly (Table S5).

In addition to the differences in coupling strength, we checked for differences in coupling phase between N2 and N3 sleep depths. SO-slow spindle coupling phases were significantly closer to 180° (SO negative half-wave peak, i.e., SO trough) in N2 than N3, over all electrodes in both conditions (Figures 2A–2C, cluster-based permutation test, $p = 0.001$ and $p = 0.003$ for No Task and Task conditions, respectively). Fast

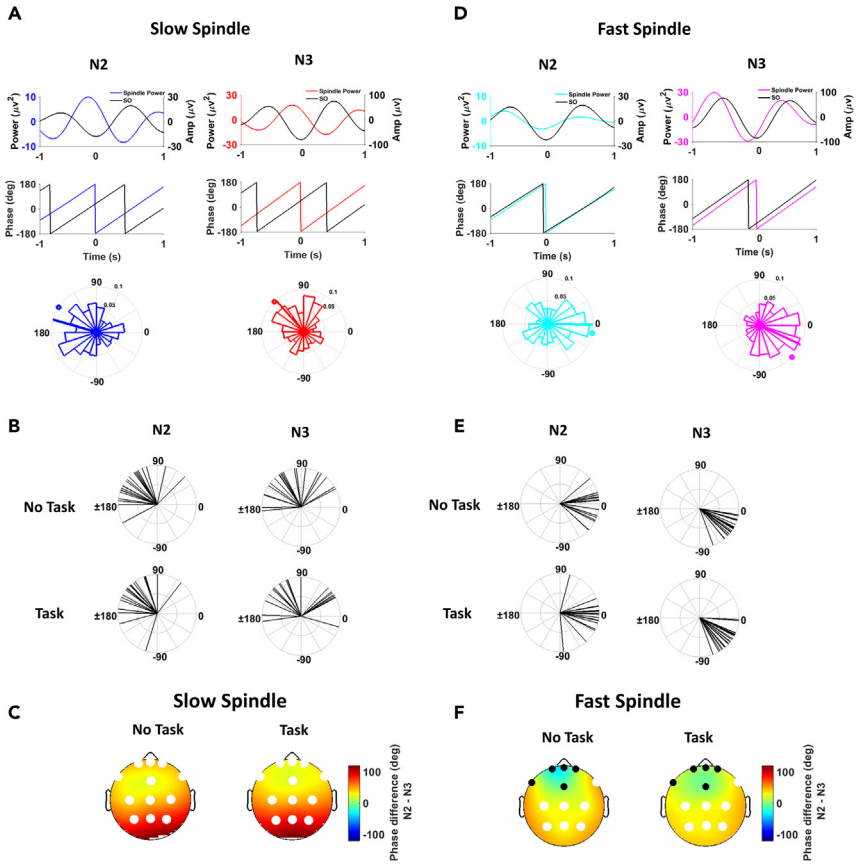

Figure 2. Differences in SO-spindle coupling between N2 and N3 sleep depths

(A) Top: EEG (black) and slow spindle power filtered in 0.5–1.25 Hz time-locked to negative half-wave peak (t = 0 s) of one exemplary SO event in N2 (blue) and N3 (red) for Task condition, for Fz. Middle: the phases of both signals obtained using the Hilbert transform showing a phase shift of 147.02° and 114.96° for N2 and N3 respectively. Bottom: Distribution of the phase shifts (SI angles) for all SO events for one exemplary subject. The solid line shows the mean SO-spindle coupling phase. The phase shifts corresponding to the exemplary SO events shown above were marked by circles.

(B) Distributions of mean SO-slow spindle coupling phases in N2 (Left) and N3 (Right) in No Task (Top) and Task (Bottom) conditions for Fz electrode for all subjects. Mean ± SEM across all subjects of SO-slow spindle coupling phases at Fz in N2 and N3 in the No Task and Task conditions: No Task, N2, phase = 139.81 ± 6.68°; N3, 113.62 ± 8.62°; Task, N2, phase = 137.02 ± 7.31°, N3: 97.54 ± 10.45°.

(C) Topographical distribution of SO-slow spindle coupling phase difference between N2 and N3 in No Task (Left) and Task (Right) conditions for all subjects. Significant clusters were identified over all electrodes for both No Task and Task conditions (cluster-based permutation test, slow spindle: $p = 0.001$ and $p = 0.003$ for No Task and Task respectively). $p < 0.05$, white electrodes, $p > 0.1$, black electrodes for comparisons between N2 and N3 (circular m-test).

(D) Same as (A) for SO-fast spindle coupling for Cz. Phase shifts of −11.62° and −35.23° for N2 (cyan) and N3 (magenta) respectively.

(E) Same as (B) for SO-fast spindle coupling phases for the Cz electrode. Mean ± SEM across all subjects of SO-fast spindle coupling phases at Cz in N2 and N3 in the No Task and Task conditions: No Task, N2, phase = −4.62 ± 4.68°, N3: −34.42 ± 2.73°; Task, N2, phase = −7.67 ± 5.94°, N3, -36.97 ± 3.23°).

(F) Same as (C) for the SO-fast spindle coupling phase difference. Significant clusters were identified over centro-parietal electrodes (F8, C3, Cz, C4, P3, Pz and P4) for both No Task and Task conditions (cluster-based permutation test, $p = 0.004$, $p = 0.003$ for No Task and Task respectively).

spindles at centro-parietal electrodes coupled significantly closer to the SO positive peak (0°) also in N2 than in N3, in both conditions (Figures 2D–2F, cluster-based permutation test, $p = 0.004$ and $p = 0.003$ for No-Task and Task conditions, respectively).

Slow oscillations-slow spindle coupling in N2 is stronger for subjects with higher memory quotient in the task condition

We next conducted a repeated measures ANCOVA for spindle properties with Stage and Topography as two within-subject factors and memory quotient (MQ) as a covariate to investigate their association with MQ. The ANCOVA for SO-slow spindle coupling strength revealed a significant interaction of Stage with MQ ($F(1,22) = 4.31$; $p = 0.049$), yet only in the Task condition. To better understand this interaction, we calculated correlation between MQ and SO-slow spindle coupling strength in N2 and N3. SO-slow spindle coupling strength was positively correlated with MQ in N2 for Task condition at FP1, FPz, F7, Fz,F8, C3, Cz, C4, P3 and P4 electrodes (cluster-based permutation test, $p = 0.008$; Figure 3). Subjects with higher MQ revealed stronger SO-slow spindle coupling strength. There was no significant correlation between MQ and SO-slow spindle coupling strength in N3.

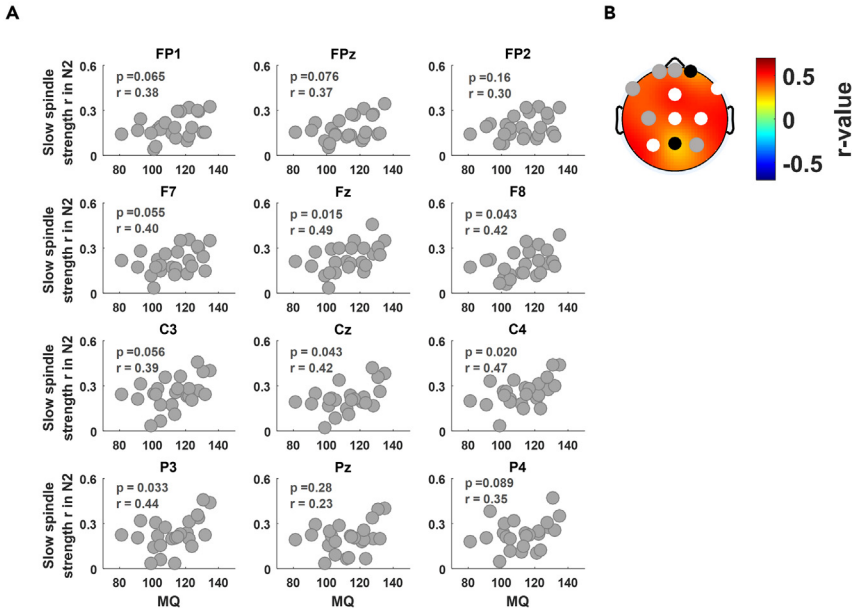

Figure 3. SO-slow spindle coupling is stronger for subjects with higher general memory quotient (MQ) in N2 in the Task condition

(A) Scatterplots for Spearman correlation between SO-slow spindle coupling strength and MQ for the Task condition in N2.

(B) Topographical distribution of the Spearman correlation between SO-slow spindle coupling strength and MQ. Electrodes belonging to the cluster (FP1, FPz, F7, Fz, F8, C3, Cz, C4, P3 and P4) revealing a significant correlation for Task in N2 (cluster-based permutation test, $p = 0.008$) are indicated by white ($p < 0.05$) and gray ($0.05 < p < 0.1$) dots. $p > 0.1$, black dots.

Slow spindle density only tended to negatively correlate with MQ in N2 only for No Task over frontal electrodes ($p = 0.052$, cluster-based permutation test, $F(11,242) = 4.18$, $p = 0.053$ for MQ × Topography interaction, repeated measures ANCOVA). There were no significant effects of MQ or its interactions on slow spindle power nor on fast spindle measures ($p > 0.1$).

We anticipated that there may also be relationship between SO-slow spindle coupling phase, especially in N2 and MQ. However, as revealed in Figure 4, there was only a tendency of MQ to correlate with SO-slow spindle coupling phase, with high MQ subjects coupling closer to the SO trough (180°) over center-left frontal electrodes only in N3 for the Task condition (Figure 4C, cluster-based permutation test, $p = 0.073$ for Fp1, Fpz and F7). SO-fast spindle coupling measures also failed to correlate significantly with MQ.

Correlations of overnight retention with spindle properties

We explored first the correlation between spindle power and density for all subjects, yet separately for N2 and N3, and overnight retention (in the Task condition; Figure S2). The FPA task retention performance correlated positively with fast spindle density in N2 over wide spread prefrontal to parietal regions (FP1, FPz, FP2, Fz, C3, Cz, C4 and Pz, cluster-based permutation test, $p = 0.013$, Figures 5A and 5B). Interestingly in N3, FPA and 2DL retention performance correlated negatively with fast spindle power over clusters at FP1, FPz, F7, Fz, F8, C3,Cz, C4, Pz for FPA task and at a cluster including more parietal regions for 2DL the task (FP1, FPz, FP2, F7, Fz, F8, C3, Cz, C4, P3, Pz, P4 cluster-based permutation test, FPA: $p = 0.028$, 2DL: $p = 0.011$, Figures 5C and 5D). Retention performance on the declarative memory tasks did not correlate with either of these slow spindle measures and performance on the procedural memory tasks only tended to correlate with a few spindle measures ($p > 0.06$): MT error only tended to negatively correlate with both fast and slow spindle power in N2 and N3 (cluster-based permutation test, fast spindle: $p = 0.069$, $p = 0.06$ for N2 and N3 respectively, slow spindle: $p = 0.076$, $p = 0.072$ for N2 and N3 respectively). In addition, MT speed tended to positively correlate with slow spindle density in N2 (cluster-based permutation test, $p = 0.06$).

We next investigated the correlation between the SO-spindle coupling strength and memory retention for both slow and fast spindles, separately for N2 and N3. At both sleep depths, MT error correlated negatively with SO-fast spindle coupling strength at frontal, extending to central electrodes (see Figures 6A and 6D, cluster-based permutation test, $p = 0.016$, and $p = 0.034$ for N2 and N3 respectively). Moreover, FST speed correlated positively with SO-fast spindle coupling strength only in N2 at fronto-central sites (see Figure 6A, cluster-based permutation test, $p = 0.035$; Figure 6A). Electrodes for the correlation diagrams in Figure 6B and 6D were selected on theoretical grounds, over regions where enhanced neural activity could be expected: contralateral to the performing hand (C4) for accuracy and speed and associated with performance monitoring (F7) for error. Retention performance of the declarative memory tasks did not correlate significantly with SO-fast spindle coupling strength nor did any correlation exist between SO-slow spindle coupling strength and memory retention of either declarative or procedural memory tasks ($p > 0.06$).

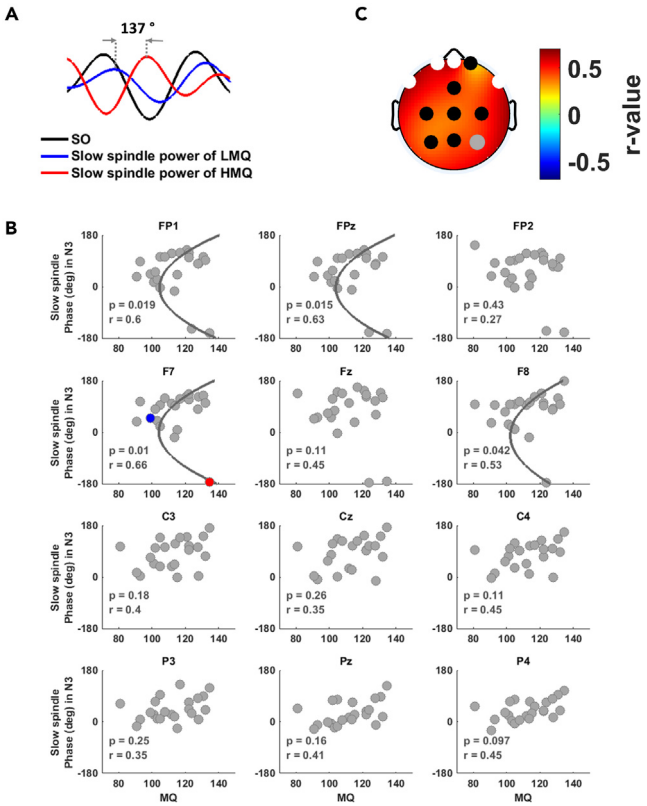

Figure 4. SO-slow spindle coupling phase for higher MQ subjects is closer to the SO trough in N3 in the Task condition

(A) Slow spindle wavelet power (obtained from TFR) time-locked to the SO negative half-wave peak (SO trough) for one exemplary low (LMQ, blue line, MQ = 99) and one exemplary high MQ subject (HMQ, red line, MQ = 135) for F7. The SO-slow spindle coupling phase is 49.26° (n = 992 SOs) and −173.60° (n = 1050 SOs) for the low and the high MQ subjects, respectively, resulting in a phase difference (low MQ – high MQ) of −137.14°. This negative phase difference indicates that the slow spindle power of high MQ subject leads the one of the low MQ subjects.).

(B) Circular-linear correlation diagrams between SO-slow spindle coupling phase and MQ for all electrodes. To further visualize nonlinear circular-linear relationship for the significant correlations a quadratic fit is shown by black solid curve. Red and blue dotes correspond to the same subjects shown in (A).

(C) Topographical distribution of circular-linear correlation between SO-slow spindle coupling phase and MQ in Task condition for N3. A cluster was identified over the frontal region (FP1, FPz and F7) after the Task but did not reach significance (p = 0.073, nonparametric cluster-permutation statistics).

Overall, our results indicated that while the SO-slow spindle coupling was associated with the general memory quotient, fast spindle power, density and SO-fast spindle coupling strength were correlated with overnight memory consolidation.

Predictive value of spindle properties

Our final set of analyses investigated the predictive capacity of fast and slow spindle properties during each NREM sleep stage, N2 and N3, as well as subjects' sex and age for both general memory ability and memory consolidation. Based on the frequently observed topographical gradient in spindle properties between fronto-central and parietal regions we focused only on fronto-central electrode locations (FP1, FPz, FP2, F7, Fz, F8, C3, Cz, C4) as multiple predictors in the generalized linear models (GLM) for MQ score and memory consolidation of the different tasks. In addition, slow oscillations possess maximal amplitude distributions at anterior locations. Analyses were conducted separately for N2 and N3.

Slow spindle properties are predictive of memory quotient

Figure 7A reveals the performance of the general linear model (GLM), regarding the relationship to MQ. The predictive error for the testing data of MQ (different from the training data; see STAR methods for details) was significantly lower when slow spindle properties (coupling, power and density) in N2 of the Task condition were used as regressors (main effects of Condition: $F(1,275) = 38.81$, $p < 0.001$; Stage: $F(1,275) = 4.23$, $p = 0.039$; and interaction Condition X Stage: $F(1,275) = 17.98$, $p < 0.001$). Table 1 reveals the GLM-derived coefficients for the slow spindle properties computed separately for the two conditions and stages. Notably, here only SO-slow spindle coupling strength and slow spindle density of the Task condition in N2 were associated with MQ. Our data did not provide any effect for fast spindle properties on MQ using the GLM model (Table S6).

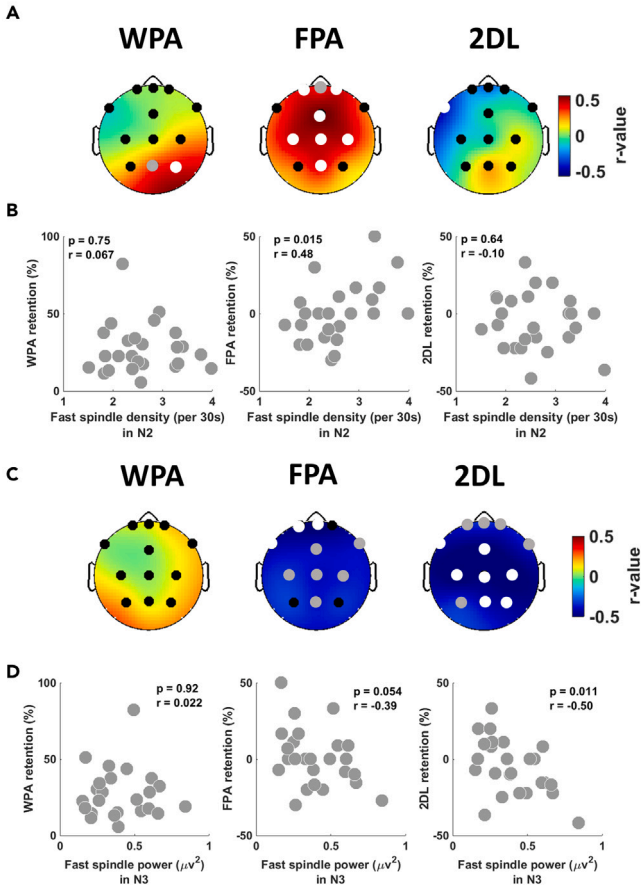

Figure 5. Differential correlations of overnight retention with N2 and N3 for fast spindle activity

(A) Topographical distribution of the coefficients r for correlations between the retention on the WPA (Left), FPA (Middle) and 2DL (Right) tasks and fast spindle density in N2. A significant cluster was identified over FP1, FPz, FP2, Fz, C3, Cz, C4 and Pz for the FPA task only (cluster-based permutation test, $p = 0.013$).

(B) Correlation diagrams for Cz between the retention of the WPA (Left), FPA (Middle) and 2DL (Right) tasks and fast spindle density in N2.

(C) Same as (A) but for fast spindle power in N3. Significant clusters were identified over FP1, FPz, F7, Fz, F8, C3,Cz, C4, Pz electrodes for FPA task and over FP1, FPz, FP2, F7,Fz, F8, C3, Cz, C4, P3, Pz and P4 electrodes for 2DL task (cluster-based permutation test, FPA: $p = 0.028$, 2DL: $p = 0.011$).

(D) Same as (B) but for fast spindle power in N3. For dots in A and C: $p < 0.05$, white electrodes; $0.05 < p < 0.1$, gray electrodes; $p > 0.1$, black electrodes (Spearman correlation). For filled circles in B and D, each circle represents a subject. WPA, word paired associate task, FPA, figural paired associate task, 2DL, 2D-object location task.

Fast spindle density and power are predictive for memory consolidation

We next applied the GLM to quantify any contribution of fronto-central spindle properties in predicting retention on the declarative memory tasks. The GLM with sex, age, mean SO-spindle coupling strength, spindle power, and density of FP1, FPz, FP2, F7, Fz, F8, C3, Cz, C4 as the predictor variables and retention as a response variable revealed a significant effect of fast spindle density in N2 for FPA retention (Figure 7B). Comparison of the GLM coefficients corresponding to fast spindle density in stages N2 and N3 among different tasks revealed that the coefficient estimate was significantly larger, for the FPA task, in N2 than N3 (Figure 7B; Stage: $F(1,275) = 1024$, $p < 0.001$; Task: $F(2,550) = 3676$, $p < 0.001$; Stage X Task: $F(2,550) = 1806$, $p < 0.001$).

GLM-derived beta coefficients for fast spindle power in stages N2 and N3 revealed above chance effects for FPA in N2 and 2DL in N3 (Figure 7B). In both cases decreased fast spindle power was associated with increased retention (Stage: $F(1,275) = 182.9$, $p < 0.001$; Task: $F(2,550) = 7175$, $p < 0.001$; Stage X Task: $F(2,550) = 2310$, $p < 0.001$). We found no significant effect of slow spindle properties for retention performance on the declarative memory tasks (Table S7).

For the prediction of the retention on procedural memory tasks, the GLM revealed a significant effect of fast spindle power in N2 and N3 for MT speed, and a significant effect of fast spindle power and density in N3 for MT error and speed respectively (Table S8). Age was also predictive of MT error and speed. An increase in age was associated with increased MT errors and decreased MT speed.

We found a significant effect of slow spindle power only for MT speed in N2 using the GLM model (Table S9).

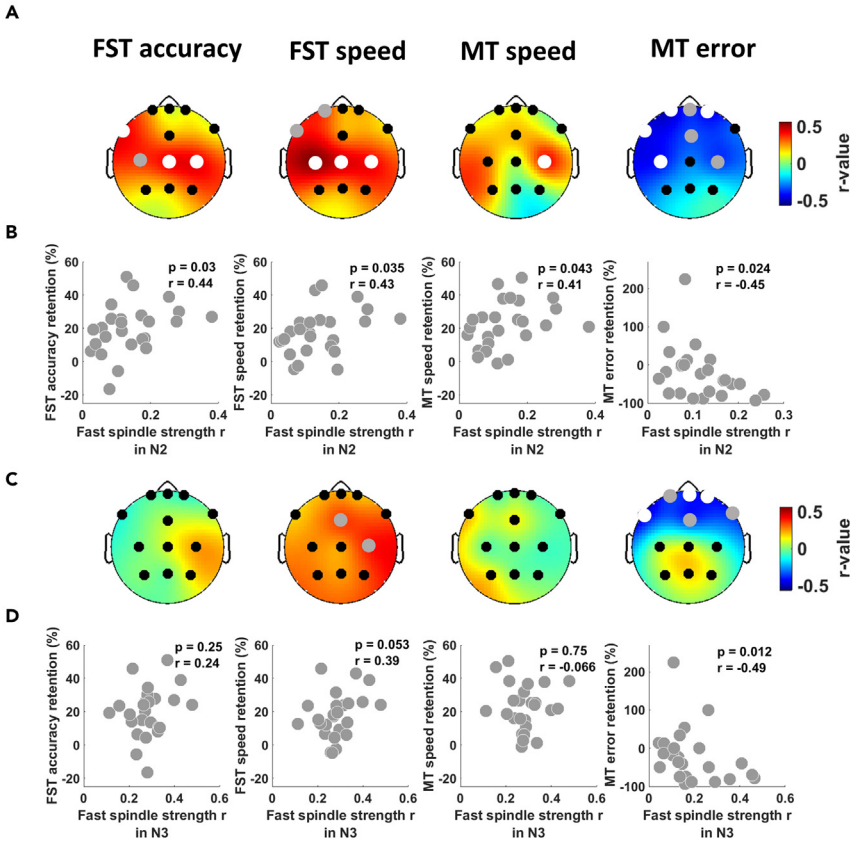

Figure 6. Association between SO-fast spindle coupling strength and procedural memory retention

(A) Topographical distribution of the correlation coefficients r between the measures of retention performance on the procedural memory tasks and SO-fast spindle coupling strength in N2. Significant clusters were identified for FST speed over FP1, F7, C3, Cz, C4 and for MT error over FP1, FPz, FP2, F7, Fz, C3, C4 (cluster-based permutation test for MT error: $p = 0.016$; FST speed: $p = 0.035$). There was only a tendency of FST accuracy to correlate with SO-fast spindle coupling strength over F7, C3, Cz, C4 (cluster-based permutation test, $p = 0.078$).

(B) Corresponding correlation diagrams between retention performance and SO-fast spindle coupling strength in N2 for C4 (for FST accuracy, FST speed and MT speed), and F7 (MT error).

(C and D) Same as (A) and (B) respectively but for SO-fast spindle coupling strength in N3. A significant cluster was identified only for retention for MT error over FP1, FPz, FP3, F7, Fz, F8 (cluster-based permutation test, $p = 0.034$). $p < 0.05$, white electrodes; $0.05 < p < 0.1$, gray electrodes; $p > 0.1$, black electrodes.

Taken together, the present results underscore and extend our above findings by showing that following a declarative memory task, conjoint slow spindle properties in N2 were predictive for subjects' MQ. On the other hand, fast spindle density and power were associated with overnight memory retention.

DISCUSSION

Recently, interest in the differential physiological differences between depths of NREM sleep, especially of N2 and N3,[12,28,51,52] and the spatiotemporal dynamics of SOs and between SOs and spindles[23,30,31] have increased. The present data compliment and extend these findings by looking into spindle properties of N2 and N3 sleep relating to general memory ability and memory consolidation. Specifically, our main and novel finding reveals the predictive value of combined slow spindle properties in post–task N2 sleep for subjects' MQ. Or vice versa, that the MQ measure of general memory ability of a subject is best reflected by conjoint slow spindle properties (SO-spindle, coupling, density, power) in N2 sleep and after conducting a battery of memory tasks. Our findings provide, for our set-up, the functional relevance of slow spindles (~9–12 Hz). In the meta-analyses by Ujma[47] in which overall assessment did not permit to distinguish between depth of NREM sleep or type of mental ability, slow spindle amplitude and moderately density were associated with general cognitive ability. The authors also found an association for fast spindle amplitude, which was however not found here. Our results emphasizing the relevance of spindles in N2 sleep are in line with previous reports showing a tendency of slow spindles in N2 to be positively related to other trait-like measures, such as the working memory subdomain of fluid intelligence (ADRA) and a strong tendency of N2 spindles to be increased in subjects performing good on the Wechlser Memory Scale-revised or a similar intelligence test.[36,46,53] Although MQ does not equate with these IQ scores its subtests rely partly on overlapping capacities and functional networks.[46] The relevance of NREM sleep depth is interesting in lieu of the

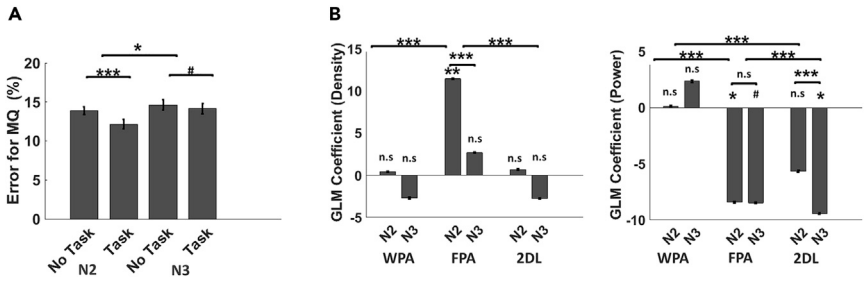

Figure 7. Predictive properties of spindles: GLM performance

(A) Accuracy of the MQ prediction using the GLM model with all three slow spindle properties as regressors on test data indicates an enhanced prediction of MQ when the slow spindle properties in N2 of the Task condition were used. Data are given as error of MQ prediction (mean ± SEM) for the testing data averaged across 276 training-testing iterations (*$p < 0.05$, rm ANOVA; ***$p < 0.001$, # $0.05 < p < 0.1$, paired t-test).

(B) Comparison of the GLM-derived coefficients (mean ± SEM) of fast spindle density (left) and power (right) for retention in the WPA, FPA and 2DL tasks. rm ANOVA revealed a significant effect of both Stage (N2, N3), Task (WPA, FPA, 2DL) and interaction of Task X Stage for fast spindle density. rm ANOVA revealed a significant effect of Task, Stage and interaction of Task X Stage for fast spindle power, cp. text. (***$p < 0.001$, paired t-test; **$p < 0.01$, *$p < 0.05$, # $0.05 < p < 0.1$, n.s. $p > 0.1$, one sample t-test). WPA, word paired associate task, FPA, figural paired associate task, 2DL, 2D-object location task.

differential network dynamics described by others. For instance, EEG and fMRI studies indicate that degree of brain functional connectivity decreases from light to deep NREM sleep[25,54] and N2 is characterized by more stable cortical-subcortical networks than N3.[30] Activity reflecting trait-like properties as MQ could be presumed to arise more likely from a network of greater stability.

Notably, within N2 prediction accuracy of compound slow spindle properties for MQ was higher for the Task than No Task condition. This distinction reflects an interaction between a mental ability score and learning induced activity, as previously observed.[46] Those authors concluded from relationships between sleep spindles in N2 and tests that spindles reflect important aspects of efficient cortical-subcortical connectivity and are thus linked to general cognitive-as well as memory-related abilities. SO-spindle coupling was not measured in that study. The fact that in N2, SO-slow spindle coupling strength across broad topographical regions was the strongest positive predictor variable for MQ (Figure 3, Table 1) agrees to the upheld functional connectivity in N2 as mentioned above. Interestingly, our data also reveal the novel finding that slow spindle density was a significant, albeit negative predictor of MQ.

On the other hand, fast spindle density and power were related to memory retention (Figure 5). In line with expectations reviewed in[5,40] our results on fast spindle density revealed a positive correlation with overnight retention (on the FPA task) in N2, the sleep stage in humans with the highest fast spindle density.[55] This agrees with observed stronger functional connectivity between subregions of the hippocampal formation and cortical regions in N2 over N3.[56] Unexpectedly, in N3 we observed a negative correlation between fast spindle power and retention for FPA and 2DL. We speculate this decrement to be linked in some way to a homeostatic network activity, since individual electrodes revealing this negative correlation between retention and fast spindle power appear to overlay regions potentially more strongly involved in these tasks (left frontal for the relatively demanding FPA, and centro-parietal for the spatial 2DL; Figure 5B). Such opposite correlations between performance and spindle power in N2 and N3 sleep was previously reported for spindle activity during sleep after a task of memory forgetting 58. A biological distinction between light as compared to deep NREM sleep which could open several windows for further investigation is the finding of increased regional cerebral protein synthesis in light as compared to deep NREM sleep in humans.[58]

We found that SO-fast spindle coupling strength was stronger in N3 than N2. Yet, fast spindles coupled to an earlier phase on the rising phase of the SO Up state in N3 than N2 (in both conditions). How could the close relationship between increased retention performance and fast spindle density in N2 on the one hand, yet stronger SO-fast spindle coupling, coupling to an earlier phase and negative correlation between fast spindle power and retention in N3, on the other hand, be reconciled? The occurrence of fast spindles at an earlier phase of SO up

Table 1. Results for the GLM with slow spindle properties as predictor variables for MQ

	N2	N2	N2	N2	N3	N3	N3	N3
	No Task	No Task	Task	Task	No Task	No Task	Task	Task
Slow spindle properties	β	p	β	p	β	p	β	p
Strength r	3.53	0.23	5.97	0.03 *	−1.21	0.74	2.14	0.53
Power	0.69	0.82	−1.58	0.56	0.16	0.96	0.09	0.98
Density	−4.88	0.13	−6.15	0.03 *	−1.43	0.71	−1.8	0.61
Sex	5.15	0.09	5.08	0.07	5.42	0.11	5.62	0.11
Age	0.53	0.87	0.12	0.96	3.3	0.32	3.15	0.34

The coefficients and p values of the GLM model with slow spindle properties over FP1, FPz, FP2, F7, Fz, F8, C3, Cz, and C4 electrodes as well as sex and age as predictor variables for MQ. GLM was separately conducted for each condition and stage, *$p < 0.05$.

state in old adults compared to the coupling of fast spindles around SO peak in young adults was suggested to be associated with age-related impairments in overnight memory retention.[59] Coupling at the unfavorable phase was interpreted as decreased precision in coordinated spindle-related and hippocampal activity. Indeed, using intracranial electrodes in patients Jiang et al. discovered more frequent coupling of neocortical graphoelements to hippocampal SPWR in N2 than in N3, despite increased SPWR density in N3.[60] Thus, functional distinctions we find between N2 and N3 may be related differences in SO-SPWR coupling.

The function of SO is still a matter of debate. Aside from the concept of SO grouping thalamic-cortical activity and hippocampal activity to serve memory reactivation and memory consolidation, large slow waves of deep NREM sleep have been associated with synaptic downscaling.[61] Thus, our data may be taken to suggest that fast spindles of deep NREM sleep serve together with slow waves a different function than during N2 spindles. It is to note, here, however, that overnight retention performance in our study was weakly expressed, reaching significance only for high MQ subjects on the FPA task. Furthermore, since subjects learned on three declarative memory tasks, processing related to spindle activity is putatively a response to multiple processing functions. Yet, our results underscore that differential processing at different NREM sleep depths occurs and encourage future studies investigating effects of learning on sleep to discriminate between activity in N2 and deep NREM sleep. This is especially important since questions as to the consistent benefit of sleep for memory consolidation have led to more fine-grained psychological concepts.[7,32,62]

A growing number of studies report in detail at the electrophysiological level on spindle properties differing between in N2 and N3 such as in their occurrence 61, timing relative to other sleep oscillations or events,[13] or on differences in their topographical distribution.[28,63] Similar dependencies of spindles within N2 and N3 on other neural activity, e.g., global vs. local SOs[23,30,31,51] and their potential molecular role[64] are also found. A number of studies have also reported predictive features of neural oscillations in sleep for memory,[32,33,37,49,65,66] and mental ability scores.[20,48] Yet studies conjointly assessing memory consolidation and NREM sleep depth as presented here are seldom.[31,52,57,67] Our results are unique in that they reveal the relationship of fast spindle activity to retention depends on task type and sleep depth. We recommend striving toward more and challenging attempts to distinguish putative differential contributions of NREM sleep sub-states to cognitive processing.

The distinctions described by us and others in brain states and neural oscillations can result from multifaceted sources including but not limited to dynamic shifts in the contributions of more hippocampal and thalamic nuclei.[68–70] Yet, such investigations on underlying mechanisms are challenging: For instance, in rodents with well pronounced hippocampal activity NREM sleep depths are less distinct than in humans; on the other hand, humans revealed an unclear degree of systematic hippocampal coupling to cortical oscillations.[60,71,72] Regarding the thalamic contributions, despite successful findings[73] far-field electrophysiological thalamic measurements are technically hampered by the non-laminar structure and electrical closed-field properties.[74]

Studies involving non-invasive brain stimulation during sleep aimed to improve memory consolidation in humans typically targeted entire NREM sleep (e.g.,.[75–78] We have previously shown that the SO-transcranial direct current stimulation efficacy depends on both general memory quotient[34] as well as the baseline sleep.[35] The results of the current study further suggest that the stimulation efficacy can also depend on the sleep stage in which the stimulation is applied.

In summary discrepancies between N2 and N3 of NREM sleep in electrophysiology or a behavioral measure have been previously reported.[12,26,28–30,57,60] The novelty of the present work is the conjoint view of slow and fast spindle measures during these two NREM sleep depths, their relationship to memory consolidation and trait-like parameter, and in addition, how previous learning effects these relationships. We find post-task SO-slow spindle coupling in N2 was a positive predictor for subjects' memory quotient, whereas SO-fast spindle coupling in N2 correlated positively with procedural retention performance. Functional correlates of spindle density differed between brain states, with slow spindle density in N2 presenting a negative predictor for MQ, and fast spindle density in N2 correlating with memory retention. Our data in N2 replicated the positive correlation between fast spindle density and memory retention, yet we also found in N3 a negative correlation of retention with fast spindle power.

We believe our findings very important in lieu of the widespread concept to improve the memory function of sleep by modulating sleep rhythms in particular sleep spindles, since our findings indicate the relevance of NREM sleep sub-states. Comparisons between intracranial local field, and global vs. local scalp EEG activity are particularly relevant at the mechanistic level. We encourage future research on sleep and memory to always distinguish the different spindle types and relationships to cognitive parameters, whereby spindle frequency ranges should be data-driven. Moreover, the predictive properties of trait-like measures for post-task brain oscillations require increased consideration in experimental designs. In the long term the sleep community would benefit greatly from increased systematic investigations, and coordination between laboratories employing scalp and intracranial recordings as well as analyses of molecular measure of neuroplasticity.

Limitations of the study

Our study has several limitations. Firstly, for comparative reasons, our analyses were limited to a 150 min interval of sleep. Thus, precluding a statement on the temporal evolution of spindle properties across sleep cycles. Thus, any overnight changes in spindle properties, e.g., frequency or effects of progressive homeostatic regulation across nocturnal sleep were not incorporated. Along these lines, our analyses window did not continue into the longer N2 sleep periods of the second part of the night, potential not including all offline consolidation processes, especially for procedural memory. Our analyses also did not distinguish between SOs coupled or uncoupled to spindles, nor on global vs. local spindles, measures which may affect cognitive relevance.[29–31] Secondly, although the test for MQ score assess a trait-like property underlying networks are presumably not independent of those required for our (declarative) memory tasks. Thirdly, we used a battery of memory tasks for comparative reasons, yet acquisition and offline consolidation may underlie interference, as thoroughly discussed in Koo et al.[34]

Finally, subjects did not receive a no-feedback final trial before sleep, so that the numeric difference in performance between morning and evening sessions cannot be solely attributed to offline consolidation.

STAR★METHODS

Detailed methods are provided in the online version of this paper and include the following:

- KEY RESOURCES TABLE
- RESOURCE AVAILABILITY
  - Lead contact
  - Materials availability
  - Data and code availability
- EXPERIMENTAL MODEL AND STUDY PARTICIPANT DETAILS
  - Participants
- METHOD DETAILS
  - Experimental design and procedure
  - General memory quotient
  - Behavioral tasks
- QUANTIFICATION AND STATISTICAL ANALYSIS
  - EEG spectral analysis and spindle peak detection
  - Slow oscillation and spindle detection
  - Phase amplitude coupling
  - Statistical analysis

SUPPLEMENTAL INFORMATION

Supplemental information can be found online at https://doi.org/10.1016/j.isci.2023.108154.

ACKNOWLEDGMENTS

We thank Erik Gromodka for support with art work. This work was supported by the BMBF grant (01GQ1706), Deutsche Forschungsgemeinschaft (MA2053/11) and the Center for International Scientific Studies & Collaborations (CISSC), Ministry of Science Research and Technology of Iran (4010118).

AUTHOR CONTRIBUTIONS

Conceptualization of study; M.G and L.M., experimental design, F.D., M.G., and L.M.; data collection, C.P.K-P.; data analysis, F.D., M.G., and C.P.K-P.; data interpretation, M.G. and L.M.; article preparation, F.D., M.G, and L.M.

DECLARATION OF INTERESTS

The authors have no conflicting interest to declare.

INCLUSION AND DIVERSITY

We support inclusive, diverse, and equitable conduct of research.

Received: March 20, 2023
Revised: August 9, 2023
Accepted: October 3, 2023
Published: October 6, 2023

REFERENCES

1. De Gennaro, L., and Ferrara, M. (2003). Sleep spindles: an overview. Sleep Med. Rev. *7*, 423–440. https://doi.org/10.1053/smrv.2002.0252.
2. Andrillon, T., Nir, Y., Staba, R.J., Ferrarelli, F., Cirelli, C., Tononi, G., and Fried, I. (2011). Sleep spindles in humans: insights from intracranial EEG and unit recordings. J. Neurosci. *31*, 17821–17834. https://doi.org/10.1523/jneurosci.2604-11.2011.
3. Marshall, L., and Born, J. (2007). The contribution of sleep to hippocampus-dependent memory consolidation. Trends Cognit. Sci. *11*, 442–450. https://doi.org/10.1016/j.tics.2007.09.001.
4. Brodt, S., Inostroza, M., Niethard, N., and Born, J. (2023). Sleep-A brain-state serving systems memory consolidation. Neuron *111*, 1050–1075. https://doi.org/10.1016/j.neuron.2023.03.005.
5. Fernandez, L.M.J., and Lüthi, A. (2020). Sleep Spindles: Mechanisms and Functions. Physiol. Rev. *100*, 805–868. https://doi.org/10.1152/physrev.00042.2018.
6. Todorova, R., and Zugaro, M. (2020). Hippocampal ripples as a mode of communication with cortical and subcortical areas. Hippocampus *30*, 39–49. https://doi.org/10.1002/hipo.22997.

7. Klinzing, J.G., Niethard, N., and Born, J. (2019). Mechanisms of systems memory consolidation during sleep. Nat. Neurosci. *22*, 1598–1610. https://doi.org/10.1038/s41593-019-0467-3.
8. Staresina, B.P., Niediek, J., Borger, V., Surges, R., and Mormann, F. (2023). How coupled slow oscillations, spindles and ripples coordinate neuronal processing and communication during human sleep. Nat. Neurosci. *26*, 1429–1437. https://doi.org/10.1038/s41593-023-01381-w.
9. Mölle, M., Bergmann, T.O., Marshall, L., and Born, J. (2011). Fast and slow spindles during the sleep slow oscillation: disparate coalescence and engagement in memory processing. Sleep *34*, 1411–1421. https://doi.org/10.5665/sleep.1290.
10. Gonzalez, C.E., Mak-McCully, R.A., Rosen, B.Q., Cash, S.S., Chauvel, P.Y., Bastuji, H., Rey, M., and Halgren, E. (2018). Theta Bursts Precede, and Spindles Follow, Cortical and Thalamic Downstates in Human NREM Sleep. J. Neurosci. *38*, 9989–10001. https://doi.org/10.1523/jneurosci.0476-18.2018.
11. Klinzing, J.G., Mölle, M., Weber, F., Supp, G., Hipp, J.F., Engel, A.K., and Born, J. (2016). Spindle activity phase-locked to sleep slow oscillations. Neuroimage *134*, 607–616. https://doi.org/10.1016/j.neuroimage.2016.04.031.
12. Cox, R., Mylonas, D.S., Manoach, D.S., and Stickgold, R. (2018). Large-scale structure and individual fingerprints of locally coupled sleep oscillations. Sleep *41*, zsy175. https://doi.org/10.1093/sleep/zsy175.
13. McConnell, B.V., Kronberg, E., Teale, P.D., Sillau, S.H., Fishback, G.M., Kaplan, R.I., Fought, A.J., Dhanasekaran, A.R., Berman, B.D., Ramos, A.R., et al. (2021). The aging slow wave: a shifting amalgam of distinct slow wave and spindle coupling subtypes define slow wave sleep across the human lifespan. Sleep *44*, zsab125. https://doi.org/10.1093/sleep/zsab125.
14. Ayoub, A., Aumann, D., Hörschelmann, A., Kouchekmanesch, A., Paul, P., Born, J., and Marshall, L. (2013). Differential effects on fast and slow spindle activity, and the sleep slow oscillation in humans with carbamazepine and flunarizine to antagonize voltage-dependent Na+ and Ca2+ channel activity. Sleep *36*, 905–911. https://doi.org/10.5665/sleep.2722.
15. Alfonsi, V., D'Atri, A., Gorgoni, M., Scarpelli, S., Mangiaruga, A., Ferrara, M., and De Gennaro, L. (2019). Spatiotemporal Dynamics of Sleep Spindle Sources Across NREM Sleep Cycles. Front. Neurosci. *13*, 727. https://doi.org/10.3389/fnins.2019.00727.
16. Del Felice, A., Arcaro, C., Storti, S.F., Fiaschi, A., and Manganotti, P. (2014). Electrical source imaging of sleep spindles. Clin. EEG Neurosci. *45*, 184–192. https://doi.org/10.1177/1550059413497716.
17. Dehghani, N., Cash, S.S., Chen, C.C., Hagler, D.J., Jr., Huang, M., Dale, A.M., and Halgren, E. (2010). Divergent cortical generators of MEG and EEG during human sleep spindles suggested by distributed source modeling. PLoS One *5*, e11454. https://doi.org/10.1371/journal.pone.0011454.
18. Marshall, L. (2020). A Role for Neuronal Oscillations of Sleep in Memory and Cognition. In Neuronal Oscillations of Wakefulness and Sleep, T.T. Dang-Vu and R. Courtemanche, eds. (Springer Science+Business Media, LLC, part of Springer Nature), pp. 192–222. https://doi.org/10.1007/978-1-0716-0653-7_7.
19. Muehlroth, B.E., Sander, M.C., Fandakova, Y., Grandy, T.H., Rasch, B., Shing, Y.L., and Werkle-Bergner, M. (2019). Precise Slow Oscillation-Spindle Coupling Promotes Memory Consolidation in Younger and Older Adults. Sci. Rep. *9*, 1940. https://doi.org/10.1038/s41598-018-36557-z.
20. Fang, Z., Sergeeva, V., Ray, L.B., Viczko, J., Owen, A.M., and Fogel, S.M. (2017). Sleep Spindles and Intellectual Ability: Epiphenomenon or Directly Related? J. Cognit. Neurosci. *29*, 167–182. https://doi.org/10.1162/jocn_a_01034.
21. Hagler, D.J., Jr., Ulbert, I., Wittner, L., Erőss, L., Madsen, J.R., Devinsky, O., Doyle, W., Fabó, D., Cash, S.S., and Halgren, E. (2018). Heterogeneous Origins of Human Sleep Spindles in Different Cortical Layers. J. Neurosci. *38*, 3013–3025. https://doi.org/10.1523/jneurosci.2241-17.2018.
22. Ujma, P.P., Hajnal, B., Bódizs, R., Gombos, F., Erőss, L., Wittner, L., Halgren, E., Cash, S.S., Ulbert, I., and Fabó, D. (2021). The laminar profile of sleep spindles in humans. Neuroimage *226*, 117587. https://doi.org/10.1016/j.neuroimage.2020.117587.
23. Stokes, P.A., Rath, P., Possidente, T., He, M., Purcell, S., Manoach, D.S., Stickgold, R., and Prerau, M.J. (2023). Transient oscillation dynamics during sleep provide a robust basis for electroencephalographic phenotyping and biomarker identification. Sleep *46*, zsac223. https://doi.org/10.1093/sleep/zsac223.
24. Genzel, L., Kroes, M.C.W., Dresler, M., and Battaglia, F.P. (2014). Light sleep versus slow wave sleep in memory consolidation: a question of global versus local processes? Trends Neurosci. *37*, 10–19. https://doi.org/10.1016/j.tins.2013.10.002.
25. Tarun, A., Wainstein-Andriano, D., Sterpenich, V., Bayer, L., Perogamvros, L., Solms, M., Axmacher, N., Schwartz, S., and Van De Ville, D. (2021). NREM sleep stages specifically alter dynamical integration of large-scale brain networks. iScience *24*, 101923. https://doi.org/10.1016/j.isci.2020.101923.
26. Cox, R., Schapiro, A.C., Manoach, D.S., and Stickgold, R. (2017). Individual Differences in Frequency and Topography of Slow and Fast Sleep Spindles. Front. Hum. Neurosci. *11*, 433. https://doi.org/10.3389/fnhum.2017.00433.
27. Vaidyanathan, T.V., Collard, M., Yokoyama, S., Reitman, M.E., and Poskanzer, K.E. (2021). Cortical astrocytes independently regulate sleep depth and duration via separate GPCR pathways. Elife *10*, e63329. https://doi.org/10.7554/eLife.63329.
28. McConnell, B.V., Kronberg, E., Medenblik, L.M., Kheyfets, V.O., Ramos, A.R., Sillau, S.H., Pulver, R.L., and Bettcher, B.M. (2022). The Rise and Fall of Slow Wave Tides: Vacillations in Coupled Slow Wave/Spindle Pairing Shift the Composition of Slow Wave Activity in Accordance With Depth of Sleep. Front. Neurosci. *16*, 915934. https://doi.org/10.3389/fnins.2022.915934.
29. Malerba, P., Whitehurst, L., and Mednick, S.C. (2022). The space-time profiles of sleep spindles and their coordination with slow oscillations on the electrode manifold. Sleep *45*, zsac132. https://doi.org/10.1093/sleep/zsac132.
30. Seok, S.C., McDevitt, E., Mednick, S.C., and Malerba, P. (2022). Global and non-Global slow oscillations differentiate in their depth profiles. Front. Netw. Physiol. *2*, 947618. https://doi.org/10.3389/fnetp.2022.947618.
31. Niknazar, H., Malerba, P., and Mednick, S.C. (2022). Slow oscillations promote long-range effective communication: The key for memory consolidation in a broken-down network. Proc. Natl. Acad. Sci. USA *119*, e2122515119. https://doi.org/10.1073/pnas.2122515119.
32. Denis, D., Mylonas, D., Poskanzer, C., Bursal, V., Payne, J.D., and Stickgold, R. (2021). Sleep Spindles Preferentially Consolidate Weakly Encoded Memories. J. Neurosci. *41*, 4088–4099. https://doi.org/10.1523/jneurosci.0818-20.2021.
33. Lustenberger, C., Wehrle, F., Tüshaus, L., Achermann, P., and Huber, R. (2015). The Multidimensional Aspects of Sleep Spindles and Their Relationship to Word-Pair Memory Consolidation. Sleep *38*, 1093–1103. https://doi.org/10.5665/sleep.4820.
34. Koo, P.C., Mölle, M., and Marshall, L. (2018). Efficacy of slow oscillatory-transcranial direct current stimulation on EEG and memory - contribution of an inter-individual factor. Eur. J. Neurosci. *47*, 812–823. https://doi.org/10.1111/ejn.13877.
35. Dehnavi, F., Koo-Poeggel, P.C., Ghorbani, M., and Marshall, L. (2021). Spontaneous slow oscillation-slow spindle features predict induced overnight memory retention. Sleep *44*, zsab127. https://doi.org/10.1093/sleep/zsab127.
36. Adra, N., Sun, H., Ganglberger, W., Ye, E.M., Dümmer, L.W., Tesh, R.A., Westmeijer, M., Cardoso, M.D.S., Kitchener, E., Ouyang, A., et al. (2022). Optimal spindle detection parameters for predicting cognitive performance. Sleep *45*, zsac001. https://doi.org/10.1093/sleep/zsac001.
37. Bastian, L., Samanta, A., Ribeiro de Paula, D., Weber, F.D., Schoenfeld, R., Dresler, M., and Genzel, L. (2022). Spindle-slow oscillation coupling correlates with memory performance and connectivity changes in a hippocampal network after sleep. Hum. Brain Mapp. *43*, 3923–3943. https://doi.org/10.1002/hbm.25893.
38. Schabus, M., Hoedlmoser, K., Pecherstorfer, T., Anderer, P., Gruber, G., Parapatics, S., Sauter, C., Kloesch, G., Klimesch, W., Saletu, B., and Zeitlhofer, J. (2008). Interindividual sleep spindle differences and their relation to learning-related enhancements. Brain Res. *1191*, 127–135. https://doi.org/10.1016/j.brainres.2007.10.106.
39. Petzka, M., Chatburn, A., Charest, I., Balanos, G.M., and Staresina, B.P. (2022). Sleep spindles track cortical learning patterns for memory consolidation. Curr. Biol. *32*, 2349–2356.e4. https://doi.org/10.1016/j.cub.2022.04.045.
40. Ulrich, D. (2016). Sleep Spindles as Facilitators of Memory Formation and Learning. Neural Plast. *2016*, 1796715. https://doi.org/10.1155/2016/1796715.
41. Peyrache, A., and Seibt, J. (2020). A mechanism for learning with sleep spindles. Philos. Trans. R. Soc. Lond. B Biol. Sci. *375*, 20190230. https://doi.org/10.1098/rstb.2019.0230.
42. Malkani, R.G., and Zee, P.C. (2020). Brain Stimulation for Improving Sleep and Memory. Sleep Med. Clin. *15*, 101–115. https://doi.org/10.1016/j.jsmc.2019.11.002.

43. Pilly, P.K., Skorheim, S.W., Hubbard, R.J., Ketz, N.A., Roach, S.M., Lerner, I., Jones, A.P., Robert, B., Bryant, N.B., Hartholt, A., et al. (2019). One-Shot Tagging During Wake and Cueing During Sleep With Spatiotemporal Patterns of Transcranial Electrical Stimulation Can Boost Long-Term Metamemory of Individual Episodes in Humans. Front. Neurosci. *13*, 1416. https://doi.org/10.3389/fnins.2019.01416.
44. Wang, B., Antony, J.W., Lurie, S., Brooks, P.P., Paller, K.A., and Norman, K.A. (2019). Targeted Memory Reactivation during Sleep Elicits Neural Signals Related to Learning Content. J. Neurosci. *39*, 6728–6736. https://doi.org/10.1523/jneurosci.2798-18.2019.
45. Wang, J.Y., Heck, K.L., Born, J., Ngo, H.V.V., and Diekelmann, S. (2022). No difference between slow oscillation up- and down-state cueing for memory consolidation during sleep. J. Sleep Res. *31*, e13562. https://doi.org/10.1111/jsr.13562.
46. Schabus, M., Hödlmoser, K., Gruber, G., Sauter, C., Anderer, P., Klösch, G., Parapatics, S., Saletu, B., Klimesch, W., and Zeitlhofer, J. (2006). Sleep spindle-related activity in the human EEG and its relation to general cognitive and learning abilities. Eur. J. Neurosci. *23*, 1738–1746. https://doi.org/10.1111/j.1460-9568.2006.04694.x.
47. Ujma, P.P. (2018). Sleep spindles and general cognitive ability – A meta-analysis. Sleep Spindles & Cortical Up States. https://doi.org/10.1556/2053.2.2018.01.
48. Bódizs, R., Kis, T., Lázár, A.S., Havrán, L., Rigó, P., Clemens, Z., and Halász, P. (2005). Prediction of general mental ability based on neural oscillation measures of sleep. J. Sleep Res. *14*, 285–292. https://doi.org/10.1111/j.1365-2869.2005.00472.x.
49. Hahn, M., Joechner, A.K., Roell, J., Schabus, M., Heib, D.P., Gruber, G., Peigneux, P., and Hoedlmoser, K. (2019). Developmental changes of sleep spindles and their impact on sleep-dependent memory consolidation and general cognitive abilities: A longitudinal approach. Dev. Sci. *22*, e12706. https://doi.org/10.1111/desc.12706.
50. Ujma, P.P., Konrad, B.N., Gombos, F., Simor, P., Pótári, A., Genzel, L., Pawlowski, M., Steiger, A., Bódizs, R., and Dresler, M. (2017). The sleep EEG spectrum is a sexually dimorphic marker of general intelligence. Sci. Rep. *7*, 18070. https://doi.org/10.1038/s41598-017-18124-0.
51. Malerba, P., Whitehurst, L.N., Simons, S.B., and Mednick, S.C. (2019). Spatio-temporal structure of sleep slow oscillations on the electrode manifold and its relation to spindles. Sleep *42*, zsy197. https://doi.org/10.1093/sleep/zsy197.
52. Wei, Y., Krishnan, G.P., Komarov, M., and Bazhenov, M. (2018). Differential roles of sleep spindles and sleep slow oscillations in memory consolidation. PLoS Comput. Biol. *14*, e1006322. https://doi.org/10.1371/journal.pcbi.1006322.
53. Fogel, S.M., Nader, R., Cote, K.A., and Smith, C.T. (2007). Sleep spindles and learning potential. Behav. Neurosci. *121*, 1–10. https://doi.org/10.1037/0735-7044.121.1.1.
54. Spoormaker, V.I., Czisch, M., Maquet, P., and Jäncke, L. (2011). Large-scale functional brain networks in human non-rapid eye movement sleep: insights from combined electroencephalographic/functional magnetic resonance imaging studies. Philos. Trans. A Math. Phys. Eng. Sci. *369*, 3708–3729. https://doi.org/10.1098/rsta.2011.0078.
55. Purcell, S.M., Manoach, D.S., Demanuele, C., Cade, B.E., Mariani, S., Cox, R., Panagiotaropoulou, G., Saxena, R., Pan, J.Q., Smoller, J.W., et al. (2017). Characterizing sleep spindles in 11,630 individuals from the National Sleep Research Resource. Nat. Commun. *8*, 15930. https://doi.org/10.1038/ncomms15930.
56. Andrade, K.C., Spoormaker, V.I., Dresler, M., Wehrle, R., Holsboer, F., Sämann, P.G., and Czisch, M. (2011). Sleep spindles and hippocampal functional connectivity in human NREM sleep. J. Neurosci. *31*, 10331–10339. https://doi.org/10.1523/jneurosci.5660-10.2011.
57. Dehnavi, F., Moghimi, S., Sadrabadi Haghighi, S., Safaie, M., and Ghorbani, M. (2019). Opposite effect of motivated forgetting on sleep spindles during stage 2 and slow wave sleep. Sleep *42*, zsz085. https://doi.org/10.1093/sleep/zsz085.
58. Picchioni, D., Schmidt, K.C., Loutaev, I., Pavletic, A.J., Sheeler, C., Bishu, S., Balkin, T.J., and Smith, C.B. (2023). Increased rates of brain protein synthesis during [N1,N2] sleep: L-[1-(11)C]leucine PET studies in human subjects. J. Cerebr. Blood Flow Metabol. *43*, 59–71. https://doi.org/10.1177/0271678x221121873.
59. Helfrich, R.F., Mander, B.A., Jagust, W.J., Knight, R.T., and Walker, M.P. (2018). Old Brains Come Uncoupled in Sleep: Slow Wave-Spindle Synchrony, Brain Atrophy, and Forgetting. Neuron *97*, 221–230.e4. https://doi.org/10.1016/j.neuron.2017.11.020.
60. Jiang, X., Gonzalez-Martinez, J., and Halgren, E. (2019). Coordination of Human Hippocampal Sharpwave Ripples during NREM Sleep with Cortical Theta Bursts, Spindles, Downstates, and Upstates. J. Neurosci. *39*, 8744–8761. https://doi.org/10.1523/jneurosci.2857-18.2019.
61. Tononi, G., and Cirelli, C. (2016). Sleep and Synaptic Down-Selection. In Micro-, Meso- and Macro-Dynamics of the Brain, G. Buzsáki and Y. Christen, eds. (Springer Copyright 2016, The Author(s)), pp. 99–106. https://doi.org/10.1007/978-3-319-28802-4_8.
62. Talamini, L.M., van Moorselaar, D., Bakker, R., Bulath, M., Szegedi, S., Sinichi, M., and De Boer, M. (2022). No evidence for a preferential role of sleep in episodic memory abstraction. Front. Neurosci. *16*, 871188. https://doi.org/10.3389/fnins.2022.871188.
63. Cox, R., Rüber, T., Staresina, B.P., and Fell, J. (2020). Phase-based coordination of hippocampal and neocortical oscillations during human sleep. Commun. Biol. *3*, 176. https://doi.org/10.1038/s42003-020-0913-5.
64. Niethard, N., Ngo, H.V.V., Ehrlich, I., and Born, J. (2018). Cortical circuit activity underlying sleep slow oscillations and spindles. Proc. Natl. Acad. Sci. USA *115*. E9220-e9229. https://doi.org/10.1073/pnas.1805517115.
65. Cowan, E., Liu, A., Henin, S., Kothare, S., Devinsky, O., and Davachi, L. (2020). Sleep Spindles Promote the Restructuring of Memory Representations in Ventromedial Prefrontal Cortex through Enhanced Hippocampal-Cortical Functional Connectivity. J. Neurosci. *40*, 1909–1919. https://doi.org/10.1523/jneurosci.1946-19.2020.
66. Hennies, N., Lambon Ralph, M.A., Kempkes, M., Cousins, J.N., and Lewis, P.A. (2016). Sleep Spindle Density Predicts the Effect of Prior Knowledge on Memory Consolidation. J. Neurosci. *36*, 3799–3810. https://doi.org/10.1523/jneurosci.3162-15.2016.
67. Watson, B.O., Levenstein, D., Greene, J.P., Gelinas, J.N., and Buzsáki, G. (2016). Network Homeostasis and State Dynamics of Neocortical Sleep. Neuron *90*, 839–852. https://doi.org/10.1016/j.neuron.2016.03.036.
68. Piantoni, G., Halgren, E., and Cash, S.S. (2016). The Contribution of Thalamocortical Core and Matrix Pathways to Sleep Spindles. Neural Plast. *2016*, 3024342. https://doi.org/10.1155/2016/3024342.
69. Hauer, B.E., Pagliardini, S., and Dickson, C.T. (2021). Prefrontal-Hippocampal Pathways Through the Nucleus Reuniens Are Functionally Biased by Brain State. Front. Neuroanat. *15*, 804872. https://doi.org/10.3389/fnana.2021.804872.
70. Adamantidis, A.R., Gutierrez Herrera, C., and Gent, T.C. (2019). Oscillating circuitries in the sleeping brain. Nat. Rev. Neurosci. *20*, 746–762. https://doi.org/10.1038/s41583-019-0223-4.
71. Cox, R., Rüber, T., Staresina, B.P., and Fell, J. (2019). Heterogeneous profiles of coupled sleep oscillations in human hippocampus. Neuroimage *202*, 116178. https://doi.org/10.1016/j.neuroimage.2019.116178.
72. Rings, T., Cox, R., Rüber, T., Lehnertz, K., and Fell, J. (2020). No evidence for spontaneous cross-frequency phase-phase coupling in the human hippocampus. Eur. J. Neurosci. *51*, 1735–1742. https://doi.org/10.1111/ejn.14608.
73. Bastuji, H., Lamouroux, P., Villalba, M., Magnin, M., and Garcia-Larrea, L. (2020). Local sleep spindles in the human thalamus. J. Physiol. *598*, 2109–2124. https://doi.org/10.1113/jp279045.
74. Buzsáki, G., Anastassiou, C.A., and Koch, C. (2012). The origin of extracellular fields and currents–EEG, ECoG, LFP and spikes. Nat. Rev. Neurosci. *13*, 407–420. https://doi.org/10.1038/nrn3241.
75. Fehér, K.D., Wunderlin, M., Maier, J.G., Hertenstein, E., Schneider, C.L., Mikutta, C., Züst, M.A., Klöppel, S., and Nissen, C. (2021). Shaping the slow waves of sleep: A systematic and integrative review of sleep slow wave modulation in humans using non-invasive brain stimulation. Sleep Med. Rev. *58*, 101438. https://doi.org/10.1016/j.smrv.2021.101438.
76. Marshall, L., Helgadóttir, H., Mölle, M., and Born, J. (2006). Boosting slow oscillations during sleep potentiates memory. Nature *444*, 610–613. https://doi.org/10.1038/nature05278.
77. Ngo, H.V.V., Martinetz, T., Born, J., and Mölle, M. (2013). Auditory closed-loop stimulation of the sleep slow oscillation enhances memory. Neuron *78*, 545–553. https://doi.org/10.1016/j.neuron.2013.03.006.
78. Ladenbauer, J., Külzow, N., Passmann, S., Antonenko, D., Grittner, U., Tamm, S., and Flöel, A. (2016). Brain stimulation during an afternoon nap boosts slow oscillatory activity and memory consolidation in older adults. Neuroimage *142*, 311–323. https://doi.org/10.1016/j.neuroimage.2016.06.057.
79. Cordi, M.J., Diekelmann, S., Born, J., and Rasch, B. (2014). No effect of odor-induced memory reactivation during REM sleep on

declarative memory stability. Front. Syst. Neurosci. *8*, 157. https://doi.org/10.3389/fnsys.2014.00157.

80. Iber, C., Ancoli-Isreal, S., Chesson, A.L., and Quan, S.F. (2007). The AASM Manual for the Scoring of Sleep and Associated Events: Rules, Terminology, and Techinical Specifications.
81. Ladenbauer, J., Ladenbauer, J., Külzow, N., de Boor, R., Avramova, E., Grittner, U., and Flöel, A. (2017). Promoting Sleep Oscillations and Their Functional Coupling by Transcranial Stimulation Enhances Memory Consolidation in Mild Cognitive Impairment. J. Neurosci. *37*, 7111–7124. https://doi.org/10.1523/jneurosci.0260-17.2017.
82. Zar, J.H. (1999). Biostatistical Analysis (Pearson Education India).
83. Maris, E., and Oostenveld, R. (2007). Nonparametric statistical testing of EEG- and MEG-data. J. Neurosci. Methods *164*, 177–190. https://doi.org/10.1016/j.jneumeth.2007.03.024.
84. Delorme, A., and Makeig, S. (2004). EEGLAB: an open source toolbox for analysis of single-trial EEG dynamics including independent component analysis. J. Neurosci. Methods *134*, 9–21. https://doi.org/10.1016/j.jneumeth.2003.10.009.
85. Oostenveld, R., Fries, P., Maris, E., and Schoffelen, J.M. (2011). FieldTrip: Open source software for advanced analysis of MEG, EEG, and invasive electrophysiological data. Comput. Intell. Neurosci.156869 https://doi.org/10.1155/2011/156869.
86. Berens, P. (2009). CircStat: a MATLAB toolbox for circular statistics. J. Stat. Software *31*, 1–21.

STAR★METHODS

KEY RESOURCES TABLE

REAGENT or RESOURCE	SOURCE	IDENTIFIER
Software and algorithm		
MATLAB 2017b	MathWorks	https://www.mathworks.com/products/matlab.html, RRID: SCR_001622
EEGLAB 13_5_4b	Delorme & Makeig[84]	https://sccn.ucsd.edu/eeglab/index.php, RRID:SCR_007292
FieldTrip 20171231	Oostenveld et al.,[85]	http://www.fieldtriptoolbox.org, RRID:SCR_004849
CircStat 2012a	Berens[86]	https://philippberens.wordpress.com/code/circstats/, RRID:SCR_016651
Others		
DC amplifier SynAmps RT	Compumedics Neuroscan, Charlotte, USA	https://compumedicsneuroscan.com/
EASYcap	EASYCAP GmbH, Herrsching, Germany	https://www.easycap.de/

RESOURCE AVAILABILITY

Lead contact

Further information and requests for resources should be directed to and will be fulfilled by the lead contact, Lisa Marshall.

Materials availability

This study did not generate any new materials.

Data and code availability

Data

All data reported in this paper will be shared by the lead contact upon request.

Code

This paper does not report original code.

All other items

Any additional information required to reanalyze the data reported in this paper is available from the lead contact upon request.

EXPERIMENTAL MODEL AND STUDY PARTICIPANT DETAILS

Participants

The details of the data used in this study were reported previously.[34] Briefly, 25 healthy subjects (female: 15, ranging from 19 to 26 years, mean age: 22.4 $\pm$ 2.12 years) participated in this study. All 25 subjects were Caucasians aside from one of Asian descent. All participants provided written informed consent signed prior to participation. The study was approved by the local ethics committee of the University of Lübeck, Germany according to the Declaration of Helsinki.

METHOD DETAILS

Experimental design and procedure

After an adaptation night, subjects participated in a non-learning baseline session (No-Task condition) and a Task session in which a battery of memory tasks was given prior to nocturnal sleep. The two sessions were separated by at least seven days with their order counterbalanced across subjects (Figure S3).

General memory quotient

General memory quotient (MQ) was assessed from a standard German Learn and Memory Test battery.[34] To obtain MQ raw scores of six subtests of learning and recall of verbal and figural content within given time limits were transformed into weighted t-value points. MQ was measured after the experimental nights, so as not to interfere with the actual memory tasks.

Behavioral tasks

Memory performance was assessed by five previously employed tasks,[34,35] three declarative (word paired-associate, WPA; figural paired-associate, FPA; 2D-object location, 2DL) and two procedural memory tasks (finger sequence tapping, FST; mirror tracing, MT). In short, the FPA task involved subjects to learn 16 figural pairs (cue-target) that were composed of geometric or non-geometric lines. Each pair was presented for 5 s on the computer monitor followed by a 1 s interstimulus interval. In immediate cued recognition subjects were prompted to indicate each target figure (intermixed with 7 other figures) upon the appearance of one cue figure. Feedback was given regardless of the subjects' response. There were no time constraints. Learning was repeated until a minimum of 10 correct answers (corresponding to 60%) during immediate cued recognition were reached. The next morning, delayed cued recognition was conducted as immediate recall in the previous evening, but without feedback. The WPA task consisted of 80 semantically related German word-pairs (cue-target), presented in two lists of 40 pairs each. The first and last three word-pairs of each list served as dummies. Sequential presentation occurred via monitor for 4 s per word pair, with 1s interstimulus interval. Immediate cued free recall of all 80 words was performed after learning, and delayed recall in the morning. For the 2D-object location task (2DL),[79] subjects were required to learn the location of 15 pairs of picture cards presented in a 5 × 6 matrix on the monitor. A 60% learning criterium was used. If subjects failed to reach the criterion, a new learning trial with a different order of objects was initiated. At immediate and delayed recall subjects were required to indicate the position of the target picture on presentation of the cue.

For the FST subjects or subjects were to type on a keyboard as quickly and accurately as possible with their non-dominant left hand a sequence of five elements (numbers from 1 to 4, e.g., 4-1-3-2-4) presented on the monitor. In the MT task subjects traced as fast and accurately as possible meaningless line-drawn figure. Only a mirror image of their hand movements and the figure were visible.

For each task, performances immediately after the learning period (prior to nocturnal sleep) and after nocturnal sleep are termed 'Learning' and 'Recall' performance, respectively. Retention was calculated as 100*(Recall performance - Learning performance)/Learning performance.

QUANTIFICATION AND STATISTICAL ANALYSIS

EEG spectral analysis and spindle peak detection

EEG were recorded from Fp1, Fpz, Fp2, F7, Fz, F8, C3, Cz, C4, P3, Pz, P4, A1 and A2 referenced to the nose (international 10:20 system) with a DC amplifier SynAmps RT (Compumedics Neuroscan, Charlotte, USA, sampling rate of 500 Hz, with a low-pass filter set at 200 Hz; a gain of 10 dB). Artifacts were removed through visual inspection of the filtered data (0.16–33 Hz). American Academy of Sleep Medicine (AASM) manual[80] was used to determine wake and sleep stages (N1, N2, N3, REM sleep) by two independent scorers. Details of determining non-overlapping slow and fast frequency ranges separately for each subject were explained previously.[35] Briefly, analyses were conducted on continuous N2 and N3 (30-s) epochs, within 150 min immediately after the termination of a sham-stimulation (i.e., commencing 46.38 $\pm$ 1.66 min after sleep onset) the power spectra (obtained by using 5 s Hanning window with 50% overlap) of the temporal derivative of EEG epochs were used to determine the fast and slow spindle peaks within the corresponding frequency range (9–11.5 Hz for slow spindles and 12.5–15 Hz for fast spindles). As reported in Koo et al.,[34] the amount of time spent in N2 (No-Task: 49.1 $\pm$ 4.2 min, Task: 48.3 $\pm$ 3.5 min) and N3 (No-Task: 65.5 $\pm$ 4.9 min, Task: 68.1 $\pm$ 4.4 min) did not differ between conditions (paired sample t-test, $p > 0.5$). Spindle peaks were determined across Fz for slow spindles, and across Cz for fast spindles for each subject. All the subjects had a discrete fast spindle peak (prominence greater than 0.02, detected from the spectra normalized with respect to power in the 0.2–4 Hz frequency band). For subjects without a prominent discrete slow spindle peak in any condition or stage, the average value for slow spindle peak frequency across other subjects was used. For subjects with slow spindle peak lower than 11 Hz, the slow spindle frequency range was determined as +/−2 Hz around the peak. For other subjects the slow spindle frequency range was determined from 2 Hz lower than the peak frequency to 12 Hz. For subjects with fast spindle peak greater than 13 Hz, the fast spindle frequency range was determined as +/−2 Hz around the peak. For other subjects, the fast spindle frequency range was determined from 12 Hz to 2 Hz greater than the peak frequency.

Slow oscillation and spindle detection

The algorithm for detecting SOs and spindles was the same as in Dehanvi et al.[35] In brief, for SO detection, first the negative and positive peaks of the filtered EEG (0.16–3.5 Hz, FIR band-pass filter, filter order corresponds to 3 cycles of the low frequency cut off, EEGLAB toolbox) were determined. Negative peaks greater than the subjects' averaged negative peak by a factor of 1.25 were detected as negative peak of slow oscillations if i) the cycle duration defined as the time between the consecutive positive to negative zero crossings was between 0.8 and 2 s and ii) the amplitude difference between the negative and positive peaks was 1.25 times larger than the averaged difference between the negative and positive peaks. Spindles were detected as intervals with the root-mean-square (RMS) of the filtered signal (individually determined spindle frequency range, FIR band-pass filter, filter order of 3 cycles the low frequency cut off) greater than 1.5 standard deviation (SD) for 0.5–3 s. RMS signal was calculated using moving windows of 0.2 s, with a step size of 10 ms and then smoothed using a moving window of 0.2 s.

Phase amplitude coupling

We assessed Phase Amplitude Coupling (PAC) between SOs and spindles like a previously employed method.[35,81] First, time–frequency Representations (TFRs) were calculated −3 s–3 s around each SO negative half-wave peak using FieldTrip toolbox of MATLAB. TFRs were then normalized as difference to pre-event baseline (−2.5 to −1.2 s) and the normalized mean power was computed in the spindle frequency range. Both EEG and the spindle power computed around the SO event were then filtered between 0.5 and 1.25 Hz (to avoid edge effects we

conducted zero-padding) and the phase difference between the SO event and spindle power were calculated using the Hilbert transform. Synchronization index (SI) is defined for each event as the circular mean of this phase difference over a time window of −1 to 1 s around the SO event.

$$SI = \frac{1}{m}\sum_{j=1}^{m} e^{i[\theta_{SO}(j) - \theta_{SP}(j)]}$$

where m is the number of time points, $\theta_{SO}(j)$ and $\theta_{SP}(j)$ are the phase value of the SO event and spindle power time series at time point t_j respectively. The absolute of SI indicates the strength of coupling between the SO and the spindle power, and the angle of SI represents the phase shift between SO event and spindle power.

Statistical analysis

MATLAB (version 2017b) was used for all statistical analyses. The data of one subject with so-slow spindle strength greater than the mean ± two times SD were excluded from all statistical analyses on slow spindle properties.

The different strengths of SO-spindle coupling strength as well as spindle density and power were tested by a two-way repeated-measure ANOVA, separately for slow and fast spindles in each condition. Stage (N2, N3) and Topography (Fp1, Fpz, Fp2, F7, Fz, F8, C3, Cz, C4, P3, Pz, P4) as two within-subject factors were used in this analysis. Next, to explore the effect of MQ on spindle properties, MQ was included as a covariate. Thereby a repeated measures ANCOVA with Stage (N2, N3) and Topography as two within-subject factors and MQ as a covariate were used. Greenhouse-Geisser corrections were applied when assumptions of sphericity were violated as indicated by Mauchly's test of sphericity. Homogenity was examined by the Levene's test and multivariate normality was assessed by calculating the Mahalanobis distance and comparing it to the Chi-square distribution. Neither criteria were violated. Analyses were conducted with SPSS statistical software version 16.

Statistical analyses on the SI angles employed MATLAB CircStat toolbox (Berens P. CircStat: a MATLAB toolbox for circular statistics.). Within-subject differences in SI phases between sleep stages N2 and N3 were tested by comparing the difference in SI angles (N2-N3) to zero using the one-sample t-test for circular values (m test in circular toolbox). The m test asks whether the population mean angle is equal to a specified value. The relationship between MQ and phase of SO-spindle coupling were investigated via circular-linear correlation (CircStat toolbox[82]). Above phase analyses were only conducted for significant SI phase distributions ($p < 0.05$, Rayleigh test number of excluded subjects for each electrode: 1 subject for F8, and P4, 2 subjects for FP1, Fz, C3, Cz, P3, and Pz and 3 subjects for FPz, F7 and C4).

The relationship between strength of SO-spindle coupling, and retention (MQ), as well as the relationship between retention (MQ) and spindle density or power, respectively were investigated via Spearman's correlation separately for slow and fast spindles. To correct for multiple comparisons for both evaluating the statistical differences and correlation analysis, a cluster-based permutation procedure like previous articles[57,83] was applied. A spatial cluster was formed as the sum of all test statistics exceeding a limit corresponding to $p = 0.1$, over the neighboring electrodes. These cluster level statistics were then subjected to a Monte Carlo permutation algorithm (1000 permutations). A similar procedure was performed for each of 1000 random permutations to establish the null distribution of cluster values. The final threshold for significance of the summed test statistic within clusters was set to $p < 0.05$. The significant clusters for the differences in spindle density, spindle power or SO-spindle coupling strength between the two stages were determined based on the t-values of paired (non-paired) t-test statistics. Clusters with significant correlations between retention (MQ) and spindle properties (density, power, SO-spindle coupling strength) were obtained using the r-values of the Spearman correlation. Clusters with significant correlations between MQ and SO-spindle coupling phase were obtained using the r-values of the circular-linear correlation.

We hypothesized that SO-spindle coupling strength, spindle power, density, as well as subject's sex and age could be predictive of MQ. So, to compute their independent contributions, we used a generalized linear model (GLM)-based estimation of MQ (glmfit function in MATLAB) with mean SO-spindle coupling strength, power, and density of FP1, FPz, FP2, F7, Fz, F8, C3, Cz, C4 during N2 and N3 as well as sex and age (in *Z* score units) as the predictor variables and MQ as a response variable with normal distribution.

One sample t-tests for each coefficient (predictors) were conducted to test the null hypothesis that the corresponding coefficient is zero against the alternative that it is different from zero, For computation of the error of the GLM model to predict MQ, two out of 24 subject datasets were selected for testing and 22 subject datasets were used for training. The averaged MQ error over the testing data was computed as:

$$MQ\ error\ = \left(\frac{1}{2}\sum_{i=1}^{2}\frac{\left|predicted\ MQ(i)\ -\ actual\ MQ(i)\right|}{actual\ MQ(i)}\right) * 100$$

For comparison of the MQ error (cp. Figure 7A), this procedure was done for 276 training-testing iterations and rm ANOVA was conducted with the main factors Condition [No Task, Task] and Stage [N2, N3].

To compute the independent contributions of SO-spindle coupling strength, spindle power, density, subject's sex and age for prediction of retention, we used regression model (or GLM model with normal distribution for response; cp. Figure 7B). Mean of SO-spindle coupling strength, spindle power and density over FP1, FPz, FP2, F7, Fz, F8, C3, Cz, and C4 electrodes during N2 and N3 as well as sex and age were the predictor variables. For fast spindle properties, 2 out of 25 subject data were selected for testing and 23 subject data were used for training. This procedure was done for 300 training-testing iterations and GLM coefficients were driven from train data and were used for rm ANOVA analysis.